This document is downloaded from the
VTT Research Information Portal
https://cris.vtt.fi

VTT Technical Research Centre of Finland

Biological contaminants analysis in microalgae culture by UV–vis spectroscopy and machine learning

Paiva, Eduardo Maia; Hyttinen, Eevi; Dönsberg, Timo; Barth, Dorothee

Published in:
Spectrochimica Acta - Part A: Molecular and Biomolecular Spectroscopy

DOI:
10.1016/j.saa.2024.125690

Published: 05/04/2025

Document Version
Publisher's final version

License
CC BY

Link to publication

Please cite the original version:
Paiva, E. M., Hyttinen, E., Dönsberg, T., & Barth, D. (2025). Biological contaminants analysis in microalgae culture by UV–vis spectroscopy and machine learning. *Spectrochimica Acta - Part A: Molecular and Biomolecular Spectroscopy*, *330*, Article 125690. https://doi.org/10.1016/j.saa.2024.125690

VTT
https://www.vttresearch.com

VTT Technical Research Centre of Finland Ltd
P.O. box 1000
FI-02044 VTT
Finland

By using VTT Research Information Portal you are bound by the following Terms & Conditions.

I have read and I understand the following statement:

This document is protected by copyright and other intellectual property rights, and duplication or sale of all or part of any of this document is not permitted, except duplication for research use or educational purposes in electronic or print form. You must obtain permission for any other use. Electronic or print copies may not be offered for sale.

Download date: 26. Mar. 2025

Spectrochimica Acta Part A: Molecular and Biomolecular Spectroscopy 330 (2025) 125690

Contents lists available at ScienceDirect

Spectrochimica Acta Part A:
Molecular and Biomolecular Spectroscopy

journal homepage: www.journals.elsevier.com/spectrochimica-acta-part-a-molecular-and-biomolecular-spectroscopy

Biological contaminants analysis in microalgae culture by UV–vis spectroscopy and machine learning

Eduardo Maia Paiva [a,*], Eevi Hyttinen [b], Timo Dönsberg [a], Dorothee Barth [b]

[a] VTT Technical Research Centre of Finland, Tekniikantie 1, 02150 Espoo, Finland
[b] VTT Technical Research Centre of Finland Ltd, Tietotie 2, P.O. Box 1000, 02044 Espoo, Finland

HIGHLIGHTS

- UV–vis absorption spectra of microalgae, flagellates and rotifers from 200 to 800 nm.
- Biopigments UV–vis absorption spectra as probes to identify flagellates and rotifers contaminating microalgae culture.
- UV–visible spectroscopy band assignment of microalgae, flagellates and rotifers based on their biopigments.
- Machine Learning spectral analysis based on PCA of ternary mixtures.
- Chemometric analysis based on score maps and loading plots from PCA.

GRAPHICAL ABSTRACT

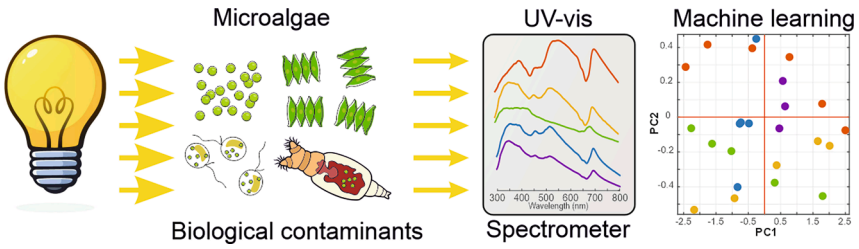

ARTICLE INFO

Keywords:
Microalgae
UV–visible spectroscopy
Machine learning
Biological contaminants
Flagellate
Rotifer

ABSTRACT

This study elucidates the utility and efficacy of UV–visible spectroscopy for the detection and characterization of biological contaminants within microalgae cultures, augmented by machine learning algorithms. Biological contamination, exemplified by flagellates and rotifers, poses a significant concern due to its potential to rapidly devastate entire cultures, thus jeopardizing commercial viability. Conventional analytical methods for monitoring contamination, such as microscopy and cytometry, are often labor-intensive, reliant on specialized expertise for microorganism identification, and may lack specificity in discerning the nature of contamination, impeding timely intervention. UV–visible spectroscopy offers a compelling solution by overcoming many of these challenges, affording specificity in analysis, real-time monitoring capabilities, and automation, owing to the intricate pigment chemistry inherent in the microalgae realm, which generates distinct UV–visible spectra. Through the measuring of contaminated and uncontaminated samples, coupled with machine learning analysis of their respective spectra, this study explores the underlying biochemical principles driving spectral data, thereby justifying the efficacy of the technique. The findings underscore the wealth of information encapsulated within UV–visible spectral data, which can be effectively harnessed through classification algorithms for early-stage identification of contamination in real-time applications.

1. Introduction

The cultivation of microalgae has been widely exploited in various commercial sectors to produce high-value chemicals essential for health, nutrition, and diverse industries including food, feed additives, dyes, cosmetics, and biofuel. Microalgae biomass generally comprises yields a

* Corresponding author.
E-mail address: eduardo.maiapaiva@vtt.fi (E.M. Paiva).

https://doi.org/10.1016/j.saa.2024.125690
Received 17 September 2024; Received in revised form 27 December 2024; Accepted 28 December 2024
Available online 2 January 2025
1386-1425/© 2024 The Author(s). Published by Elsevier B.V. This is an open access article under the CC BY license (http://creativecommons.org/licenses/by/4.0/).

wide spectrum of vital compounds, ranging from proteins, enzymes, antioxidants, lipids, and carbohydrates to carotenoids and vitamins [1]. Microalgae cultivation is an exceptional energy-effective process, harnessing sunlight as the primary energy source for cell metabolic processes. Notably, certain species such as *Chlorella* sp. produce natural edible oils that find application in infant formulas, emphasizing their nutritional importance [2]. Furthermore, the protein B-phycoerythrin sourced from *Porphyridium* showcases a myriad of biological activities, including anti-oxidative, anti-tumor, and immune-enhancing properties [3]. Also, microalgae serve as rich reservoirs of vitamins such as Vitamins A, B (including B1, B2, B3, B5, B6, B7, and B12), C, and E being richer in these nutrients than conventional vegetables [4,5]. This abundance underscores their potential as invaluable contributors to human health and various industries, promising innovative solutions and sustainable alternatives.

In general, microalgae production involves five primary stages: (1) Isolation of strains initiates the process, which entails the laborious task of collecting wild species from natural aquatic environments. Subsequently, specific cells are chosen in the laboratory using sterilized micropipettes and microscopes. (2) Cultivation follows, where biomass production occurs. This can take place in open ponds with minimal control over contamination and environmental variables such as light, nutrients, water evaporation, and temperature. Alternatively, closed photobioreactors offer a system with superior control over physical parameters, reducing contamination risks and enhancing biomass yield, albeit at a higher cost. The choice of method depends on various considerations including the desired product or location. (3) During the growth stage, light, nutrients, and environmental stressors are manipulated to maximize cell proliferation and the yield of high-value chemicals. (4) Harvesting, often the most expensive stage, involves separating cells from the aqueous medium using centrifugation, flocculation, or filtration. (5) Finally, the product is either formulated from the entire biomass or the valuable compounds are extracted through various methods tailored to the specific final product and desired purity level [6]. It is evident that the quality of the initial steps significantly influences the ease and success of achieving desired product quality during the last stages while minimizing contamination and process costs.

Biological contaminations pose a significant challenge in microalgae production due to their pervasive nature and potential to swiftly disrupt entire microalgae cultures, consequently elevating production costs [7,8]. Among the prevalent biological contaminants in *Chlorella* production are invasive microalgae, which compete for essential nutrients within the growth medium, zooplankton, known to prey on *Chlorella* as a primary food source, and bacterial and viral agents [9]. Studies indicate that bacteria possess a limited capacity to detrimentally impact overall microalgae production, while viral infections are comparatively less frequent occurrences. Of particular concern are contaminations with grazing phytoplankton, such as flagellates, and zooplankton such as rotifer, given their ubiquity, robust resistance to adverse environmental conditions, rapid growth rates, and ability to decimate microalgae cultures within a matter of days [10,11,12,13]. Special attention is warranted regarding the flagellate *Poterioochromonas malhamensis*. This mixotrophic organism sustains itself through both photosynthesis and the consumption of bacteria and microalgae. Notably, *P. malhamensis* exhibits a rapid phagocytic capacity targeting *Chlorella* cells and is inevitably present in large-scale cultivation systems. Moreover, this protozoon demonstrates resilience to harsh conditions of nutrient scarcity, salinity, and temperature fluctuations, surpassing the survivability thresholds of *Chlorella* cells. Therefore, the integration of robust characterization and analytical methods for rapid detection becomes indispensable in this context.

Analytical methods have been employed for monitoring cellular growth processes to glean insights into growth stages, phases, and the presence of contaminants [14,15]. Among the most utilized methods, non-automatic microscopic cell counting (MCC) stands out as the most intuitive approach, as it obviates the need for calibrations and facilitates direct visualization of both viable and non-viable cells and contaminants as well. However, MCC is characterized by its time-consuming nature—precluding real-time monitoring—significant labor requirements, and reliance on skilled analysts. On the other hand, optical density (OD) enables real-time monitoring of microalgae cultivation [16]. OD relies on the measurement of either light attenuation or light scattering (nephelometry) but not resolving the spectrum. OD emerges as the method of choice for monitoring microalgae growth, as it can be applied both on- and in-line using optical fibers and probes, thereby minimizing cross-contaminations—a significant concern in microalgae cultivation [17,18]. However, optical density (OD) measurements encounter challenges in accurately detecting contamination due to their nonspecific nature, as they cannot differentiate between microalgae and other particulate matter, such as debris.

Imaging techniques have been employed to monitor biological contamination during the early stages of microalgae cultivation, leveraging observations of morphology and utilizing staining strategies. However, this off-line analytical method is characterized by its sluggish pace, relatively high cost, and labor-intensive nature, rendering it impractical for monitoring large-scale production processes [19]. To streamline monitoring procedures, camera-based methods have been devised [20,15]. This approach operates under the assumption that microalgae and its biological contaminants exhibit different but regular size distributions, and they can be distinctly clustered utilizing imaging and machine learning algorithms. While effective in averting delayed interventions in microalgae production, this method faces limitations in automatically distinguishing living cells from debris and accurately identifying the type of biological contaminant, which is essential for implementing appropriate corrective measures within the culture [7,9].

Spectroscopic methods based on OD approach have exploited various wavelengths within the visible spectrum: from 400 to 680 nm (blue to red), where numerous pigments exhibit light absorption; and at 750 nm (deep red), where no pigments absorb light, resulting in “pure” scattering light. However, the OD method is subject to certain limitations, including susceptibility to light scattering across all wavelengths due to debris within the liquid solution, as well as its non-selective capability to differentiate biological contaminants from the main culture cells. Light absorption within the UV–visible spectral range (200–800 nm) primarily arises from microalgae pigments, including carotenoids, chlorophyll, and phycobiliproteins [21,22]. Notably, these biopigment are also present in other microorganisms, including phytoplankton (e.g., cyanobacteria, diatoms, and dinoflagellates) and zooplankton (e.g., rotifers). Consequently, relying solely on the OD approach may not suffice for detecting the presence of biological contamination. Alternatively, some studies have showcased the utility of Raman spectroscopy for determining cell growth phases. Raman spectroscopy offers high molecular sensitivity, enabling the detection of different species because it resolves the spectrum profile, and facilitating single-cell characterization [23]. However, the Raman spectroscopic signal encounters challenges in accurately representing the entire microalgae batch conditions due to the limited Raman sensing volume, as the laser is typically focused on a very tiny volume (few μm^3) of the sample which is required to enhance signal detection. This issue persists unless a significant number of averages are recorded, which consequently reduces the analytical throughput. Therefore, Raman spectroscopy is less suitable for extensive monitoring of large-scale microalgae production. Finally, Fourier-transform infrared spectroscopy (FTIR) also exhibits high molecular sensitivity but is impossible to apply it for monitoring living cells in aqueous solutions due to the infrared absorption of light by water.

This study presents a proof-of-concept demonstrating the potential of UV–visible spectroscopic transmittance measurements, aided by machine learning algorithms, to assess the presence of biological contaminants in early-stage microalgae production, conducted in *in-vivo* microorganisms. The experimental setup comprises a UV–visible light

source emitting wavelengths ranging from 200 to 1000 nm, a 10 mm cuvette holder, and a handheld spectrometer for acquiring full spectral data. The method was sensitive to differentiate the contaminants *Tetradesmus obliquus* (microalgae), *Poterioochromonas malhamensis* (flagellate), and *Brachionus plicatilis* (rotifer) in *Chlorella vulgaris* (main microalgae culture) bulky solution. In addition, some samples where cultured with salty medium that promotes salt stress which in turn promotes pigment misbalance that can be distinguished from those with only freshwater medium.

2. Experimental

2.1. Samples

Chlorella vulgaris CCAP211/11B, *Tetradesmus obliquus* CCAP276/3A, *Poterioochromonas malhamensis* CCAP933/1C and *Brachionus plicatilis* CCAP 5010/4 were obtained from the Culture Collection of Algae and Protozoa (CCAP) (Oban, Scotland, United Kingdom). *Chlorella* and *Tetradesmus* were cultivated in room temperature (100 rpm shaking, daylight) in modified acid medium (MAM, pH 7) [24]. *Chlorella* was additionally cultivated in MAM + 1.5 % sea salt medium, with otherwise same growth conditions. Flagellates were cultivated in 25 °C in MAM medium, no shaking, with 12/12 h light and dark cycles respectively, with daylight lamps. Rotifers were cultivated in MAM + salt medium, in the same growth conditions as the flagellates. Rotifers and flagellates were routinely fed with *Chlorella* grown in the suitable medium (MAM or MAM + salt). Cell counts in the original cultures are presented in Table 1. Microalgae cell counts were carried out with Luna-II automated cell counter (Logos Biosystems) and contaminants with manual microscopy inspections.

The samples used in the analysis are composed of a mix of the mother cultures according to Table 2. In addition, some samples were diluted with the suitable medium (MAM or MAM + salt) to obtain a range of different cell counts in the solution. Total volume of each sample was 5 ml. All samples were shaken before the measurement to avoid settling of the cells. The samples were divided into two big sample sets depending on the non-saline and saline media. Within these sample sets, the samples are further divided in smaller groups related to their components or dilution.

2.2. Uv–vis and Raman setup

The instrumental setup shown in Fig. 1 is composed of a UV–vis light source (Ocean Insight – DH-2000-BAL) that emits in the wavelength range from 200 to 1000 nm by combining deuterium and halogen lamps with balanced intensity along the spectral range. One milliliter sample fills a 10 mm optical path length cuvette (Thorlabs – CV10Q35F), which is then inserted into a cuvette holder (Thorlabs – CVH100/M) through which the transmitted light passes. The spectra were detected by a spectrophotometer (Thorlabs – CCS200/M) from 200 to 1000 nm with 2 ms exposure time per acquisition and 50 spectra average. The light from the source passes through the sample and reaches the spectrophotometer through a pair of extreme solarization-resistant optical fibers (Ocean Insight – QP600-1-XSR) with 600 μm of core diameter.

Raman spectra of the mother culture solutions were taken as shown in Supplementary Material. The spectra were taken with a picoRaman spectrometer from Timegated (Timegate, Finland), with immersion probe (Marqmetrix ball probe. Laser power 150mW, 1.5 min sample acquisition).

Table 1
Cell concentration in mother cultures post-growth.

	Microalgae/ml	Contaminant/ml
Chlorella in MAM	9.56×10^6	–
Chlorella in MAM + salt	1.24×10^7	–
Tetradesmus (MAM)	2.71×10^6	–
Flagellate (MAM)	1.06×10^7 (*Chl*)	650
Rotifers (MAM + salt)	5.31×10^5 (*Chl* + salt)	48

2.3. Data acquisition, preprocessing, and analysis

The spectral transmittance measurements were taken in triplicate and subsequently averaged. The reference spectra for absorbance calculation were taken using the cuvette filled with MAM. The spectral difference between MAM and MAM + salt was negligible.

All data preprocessing and analysis were carried out on MATLAB. For the instrumental noise smoothing, a Savitzky–Golay (SG) filter with a 51 points window and 2nd polynomial order was employed. To correct baseline shifts, four algorithms were tested: Standard Normal Variate (SNV), Asymmetric Least Squares (ALS), 1st derivative (1stDer), and Weighted Least Squares (WLS). The final performance between these baseline correction algorithms were similar and only the results with WLS are shown in this paper. The preprocessed spectral data was analyzed by Principal Component Analysis (PCA) machine learning method to explore the spectral data patterns.

3. Results

3.1. Uv–vis spectra characterization

The four organisms investigated in this study exhibited distinct UV–visible light spectral profiles attributable to variations in their biopigments. Fig. 2 illustrates these spectra acquired with the above-described setup for each individual species. Notably, discernible disparities are evident among the spectra, with *Chlorella* in non-saline medium and *Tetradesmus* exhibiting the most closely resembling profiles in terms of both profile and intensity. It is noteworthy that despite being fed with *Chlorella* during growth, the flagellate and rotifer microorganisms displayed significant spectral distinctions compared to other species. Interestingly, the spectral profiles of *Chlorella* in non-saline medium and in saline medium clearly differ from each other. *Chlorella* grown in salty medium exhibited increased absorption between 520 and 670 nm, along with a decrease around 350 nm compared to *Chlorella* grown in non-salty medium. The shaded regions in Fig. 2, denote prominent pigment absorption bands. These include the range between 620 and 740 nm, primarily governed by chlorophyll *a* and b, while phycobiliproteins exhibit absorptions around the green range (480–620 nm) [25,26,27], and numerous biomolecules, including carotenoids, chlorophylls, and minor constituents, contribute to absorption between 390 and 480 nm [28,29]. In the deep UV range (200–300 nm), absorptions arise from nucleic acids and aromatic amino acids [30], lacking specificity information for distinguishing between species. Consequently, this range was excluded from machine learning analysis and the spectral range was confined to from 300 to 800 nm. Based on the results, it is evident that the spectral range of 300–800 nm provides valuable information for the assessment of biological contaminations in microalgae cultures.

3.2. Spectral data preprocessing

Due to evident spectral disparities observed among samples cultured in saline and non-saline media, the PCA was applied to each sample set independently. The spectroscopic data depicted in Fig. 3 were subjected to smoothing by a SG filter and baseline correction utilizing the Weighted Least Squares (WLS) algorithm. This processing effectively eliminated instrumental noise and baseline drift, while preserving variances originating from chemical constituents, manifested by absorption intensities. The criterium to select the WLS method was based on its capability to preserve the spectral profiles from the original data, thereby facilitating spectroscopic interpretations.

Table 2
Mixture design of the samples that were measured with the UV–vis spectrophotometer system, denoting the amount of culture in ml that were combined to create pure, diluted or artificially contaminated samples.

Sample set	Sample #	Group	Sample code	MAM	Chlorella	Tetradesmus	Rotifer	Flagellates
No-Saline	1	1	MAM	5	–	–	–	–
	2	2	Ch5		5	–	–	–
	3		Ch4	1	4	–	–	–
	4		Ch3	2	3	–	–	–
	5		Ch2	3	2	–	–	–
	6		Ch1	4	1	–	–	–
	7		Ch.5	4.5	0.5	–	–	–
	8	3	T4	1	–	4	–	–
	9		T3	2	–	3	–	–
	10		T2	3	–	2	–	–
	11		T1	4	–	1	–	–
	12		T0.5	4.5	–	0.5	–	–
	13	4	T0.5Ch	–	4.5	0.5	–	–
	14		T1Ch	–	4	1	–	–
	15		T2Ch	–	3	2	–	–
	16		T3Ch	–	2	3	–	–
	17		T4Ch	–	1	4	–	–
	18	5	F0.5Ch	–	4.5	–	–	0.5
	19		F1Ch	–	4	–	–	1
	20		F2Ch	–	3	–	–	2
	21		F3Ch	–	2	–	–	3
	22		F4Ch	–	1	–	–	4
	23	6	T0.5Ch2MAM	2.5	2	0.5	–	–
	24		T1Ch2MAM	2	2	1	–	–
	25		T1.5Ch2MAM	1.5	2	1.5	–	–
	26		T2Ch2MAM	1	2	2	–	–
	27		T2.5Ch2MAM	0.5	2	2.5	–	–
	28	7	F0.5Ch2MAM	2.5	2	–	–	0.5
	29		F1Ch2MAM	2	2	–	–	1
	30		F1.5Ch2MAM	1.5	2	–	–	1.5
	31		F2Ch2MAM	1	2	–	–	2
	32		F2.5Ch2MAM	0.5	2	–	–	2.5
	33	8	T0.5Ch3MAM	1.5	3	0.5	–	–
	34		T1Ch3MAM	1	3	1	–	–
	35		T1.5Ch3MAM	0.5	3	1.5	–	–
	36	9	F0.5Ch3MAM	1.5	3	–	–	0.5
	37		F1Ch3MAM	1	3	–	–	1
	38		F1.5Ch3MAM	0.5	3	–	–	1.5
	39	10	T0.5Ch4MAM	0.5	4	0.5	–	–
	40	11	R0.5Ch4MAM	0.5	4	–	0.5	–
	41	12	F0.5Ch4MAM	0.5	4	–	–	0.5
Sample set	Sample #	Group	Sample code	MAM + Salt	Chl + Salt	Tetradesmus	Rotifer	Flagellates
Saline	42	1	MAMs	5	–	–	–	–
	43	13	ChS5		5	–	–	–
	44		ChS4	1	4	–	–	–
	45		ChS3	2	3	–	–	–
	46		ChS2	3	2	–	–	–
	47		ChS1	4	1	–	–	–
	48		ChS.5	4.5	0.5	–	–	–
	49	14	R0.5ChS	–	4.5	–	0.5	–
	50		R1ChS	–	4	–	1	–
	51		R2ChS	–	3	–	2	–
	52		R3ChS	–	2	–	3	–
	53		R4ChS	–	1	–	4	–
	54	15	R0.5ChS2MAMs	2.5	2	–	0.5	–
	55		R1ChS2MAMs	2	2	–	1	–
	56		R1.5ChS2MAMs	1.5	2	–	1.5	–
	57		R2ChS2MAMs	1	2	–	2	–
	58		R2.5ChS2MAMs	0.5	2	–	2.5	–
	59	16	R0.5ChS3MAMs	1.5	3	–	0.5	–
	60		R1ChS3MAMs	1	3	–	1	–
	61		R1.5ChSMAMs	0.5	3	–	1.5	–

3.3. Machine learning analysis of non-saline medium sample set

PCA was employed on the preprocessed spectral data of non-saline medium samples. The outcomes, including loadings and score maps, are depicted in Fig. 4. Fig. 4a–c illustrate the loadings of the first three PCs, while Fig. 4d and e represent the score maps for the PC1 × PC2 and PC1 × PC3 plots, respectively. Examination of the results reveals that the dominant variances pertain to *Chlorella* concentration and its dilution with MAM medium. *Chlorella* holds significant prominence in these samples, as it has a higher cell density than other organisms, as serves also as feed for the flagellate cells and to blend with *Tetradesmus* microalgae as well. The total percentage variance of each PC is showcased atop the loading plots of Fig. 4a–c. Predominant variances are manifested in both PC1 and PC2, evident in Fig. 4a, b and d. PC1 exhibits

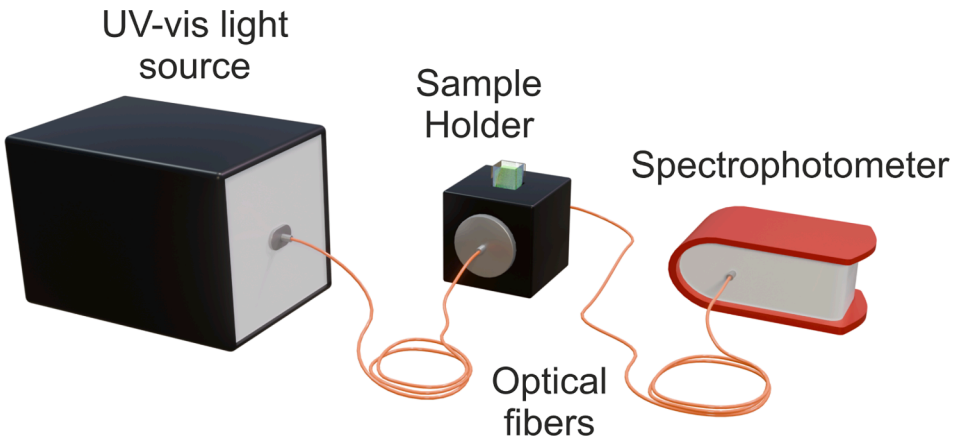

Fig. 1. Spectroscopic transmittance setup with UV–vis balanced light source, 10 mm cuvette sample holder, 200–1000 nm spectrophotometer, and optical fibers.

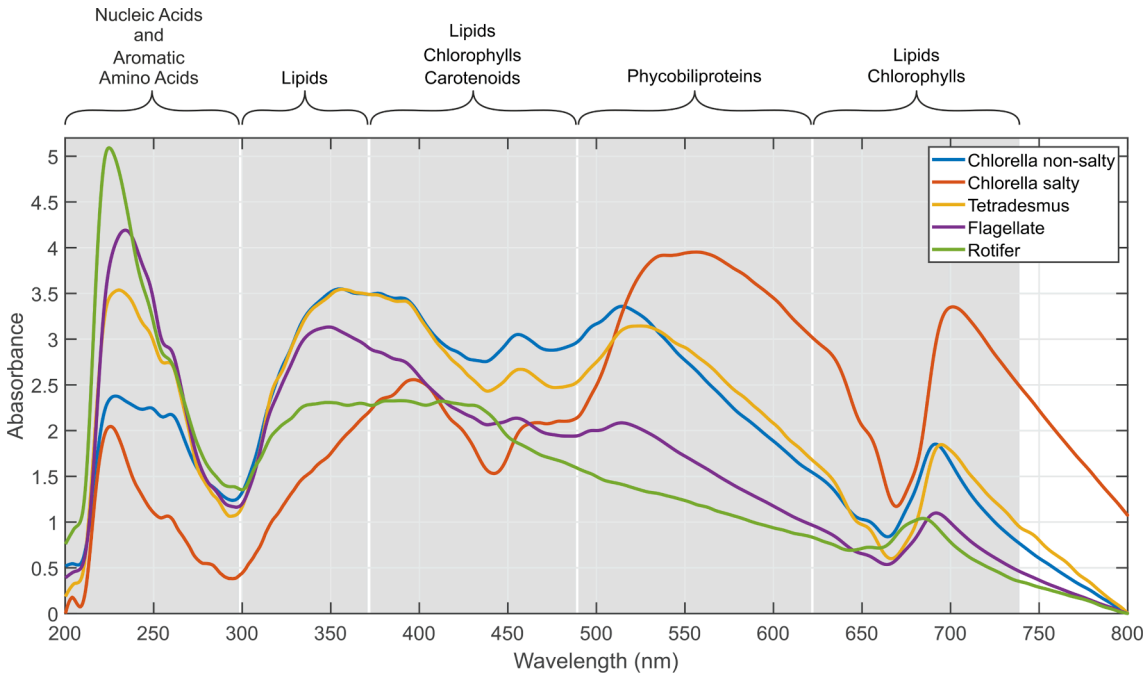

Fig. 2. UV–vis spectra of *in-vivo Chlorella vulgaris* grown in medium with and without salt, *Tetradesmus obliquus* (microalgae), *Poterioochromonas malhamensis* (flagellate), and *Brachionus plicatilis* (rotifer). The spectra were normalized to the minimum value within the range and smoothed to have a better comparison.

a profile similar to the average spectrum of this sample set. Higher concentrations correspond to more positive scores along the PC1 axis, observable across all groups within this sample set (refer to Fig. 4d).

The primary lipids found in *chlorella* microalgae are triglycerides made of oleic and palmitic acids [31] that presents large absorptions from 300 to 350 nm [32]. PC2 compile variances in the lipid (refer to the positive loadings from 300 to 350 nm in Fig. 4b [33]) plus chlorophylls (refer to the negative loadings with maximum at 520 and 692 nm in Fig. 4b [29]) concentrations. These variances in PC2 differentiated *Chlorella* appearing in the PC1xPC2 plot towards negative values and *Tetradesmus* and flagellates towards positive values (see Fig. 4d). In addition, even the smallest concentration of flagellate was sufficient to deviate the scores away from the line along the group of pure/diluted *Chlorella*, as indicated by the dashed line in Fig. 4d. The loadings in PC3 (Fig. 4c) delineate concentration variances of chlorophyll a and b, whereby a more negative position along the PC3 axis corresponds to a higher quantity of chlorophyll b relative to chlorophyll a, and vice versa. Consequently, it can be inferred that the a/b ratio between these chlorophyll pigments is greater for *Tetradesmus* microalgae than for *Chlorella*. As flagellate cells graze on *Chlorella*, their positions in the PC1xPC3 projection have intermediate scores on PC3 compared to scores of samples containing only *Chlorella*, as illustrated in Fig. 4e.

3.4. Machine learning analysis of saline sample set

The results depicted in Fig. 5 illustrate the loadings and score maps derived from PCA conducted on the saline dataset. Fig. 5a–c delineate the loadings associated with the first three PCs, while Fig. 5d and e portray the score maps corresponding to the PC1 × PC2 and PC2 × PC3 plots, respectively. The percentual of total variance explained by each PC is presented atop the loading plots in Fig. 5a–c. Predominantly, the variance observed in the dataset stems from the concentration of constituent species, notably *Chlorella*, which served as food source for the rotifers and has higher density. Consequently, PC1 primarily captures variations in *Chlorella* concentration, as its profile aligns closely with the mean spectral characteristics of the sample set. Meanwhile, PC2 reveals variances associated with lipids (refer to the negative loadings from 300 to 450 nm in Fig. 5b [33]), clustering apart rotifers and *Chlorella*. In case

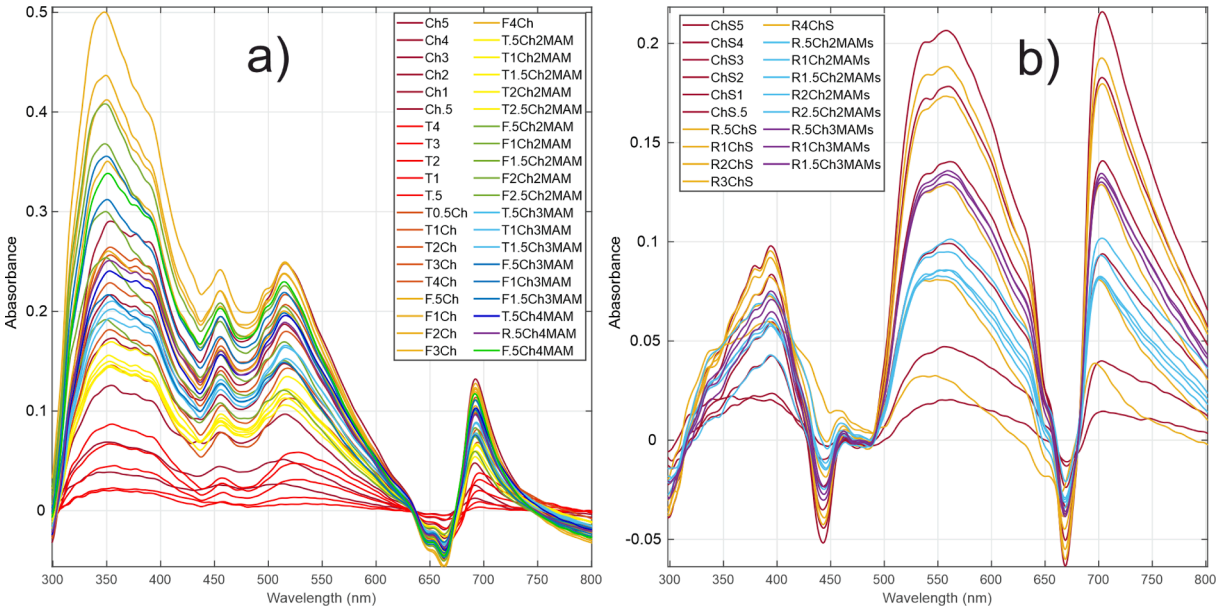

Fig. 3. Preprocessed data with SG filter for smoothing the instrumental noise and with WLS for baseline correction. (a) Samples in non-saline medium, and (b) samples in saline medium. The spectra are colored by group according to Table 2.

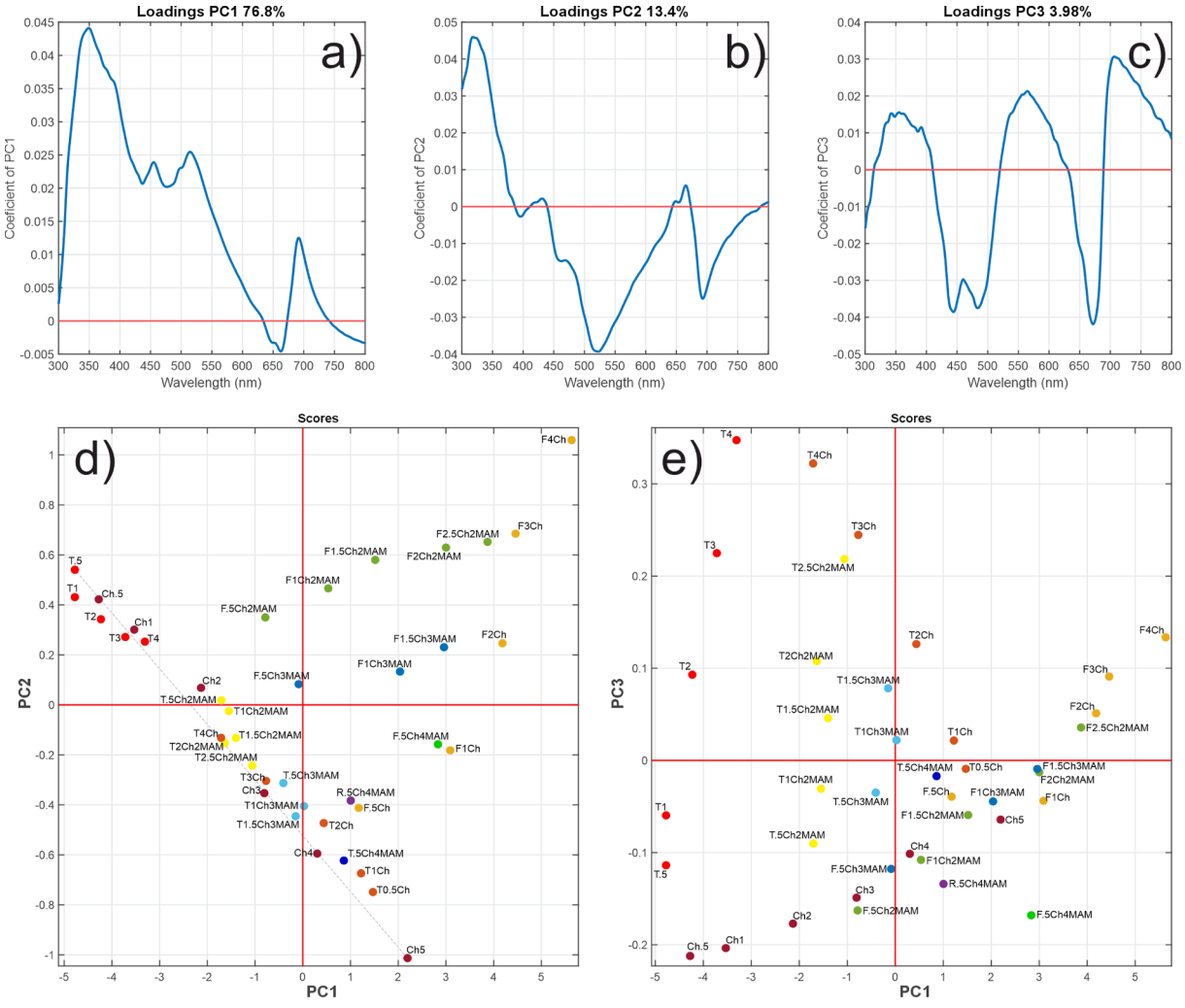

Fig. 4. Loadings (a–c) and scores (d–e) results for the PCA of with the non-saline sample set. The symbol colors represent the sample groups according to the mixture design in Table 1 and match with the spectra colors in Fig. 3a.

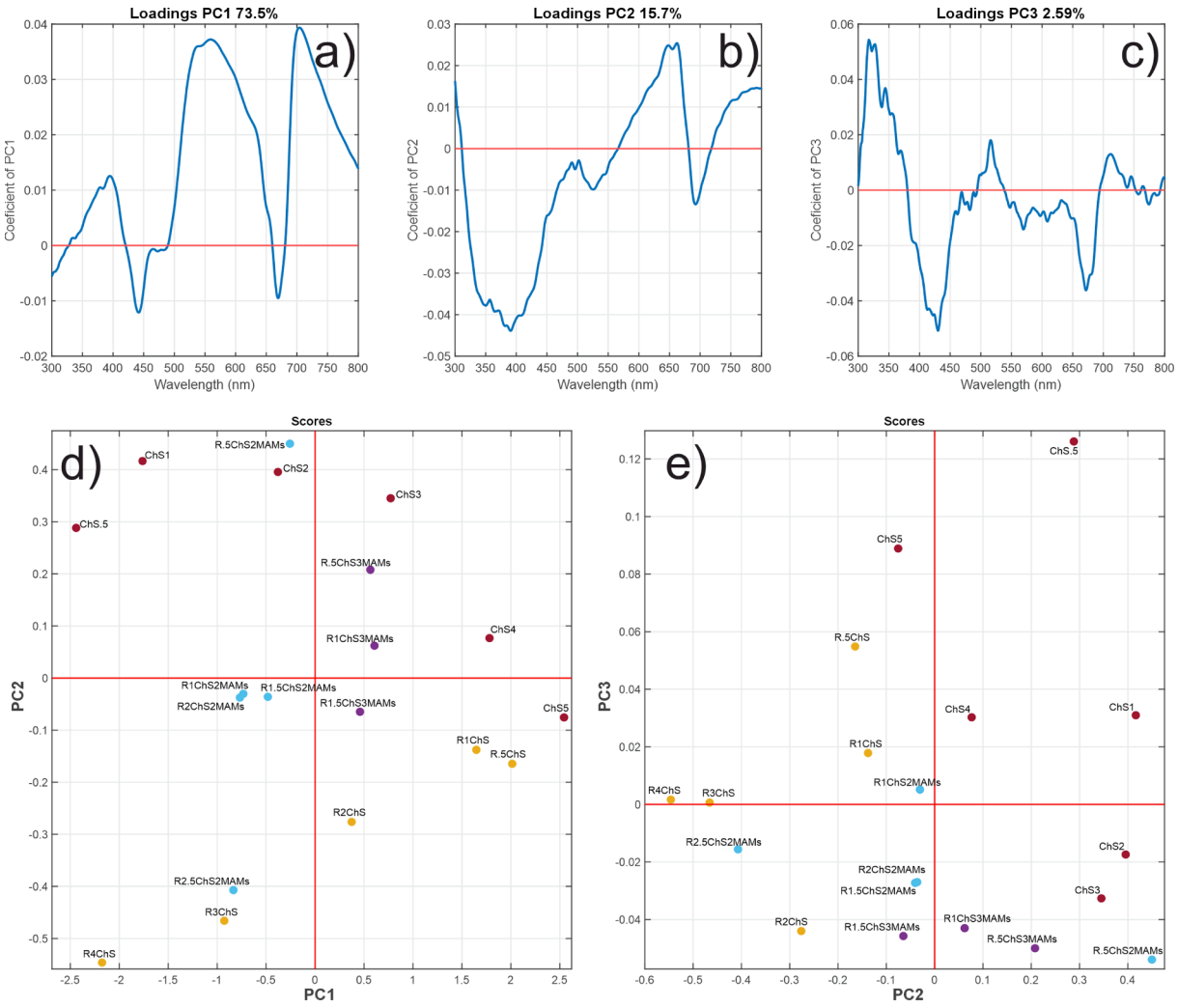

Fig. 5. Loadings (a–c) and scores (d–e) results for the PCA analysis with the saline sample set. The circle colors represent the sample groups according to the mixture design in Table 1 and match with the spectra colors in Fig. 3b.

of PC3 (Fig. 5c), the loadings match with chlorophyll absorption bands presenting negative coefficients, where rotifer are positioned (bottom-left quadrant in Fig. 5e).

4. Discussion

Microalgae, such as *Chlorella* and *Tetradesmus*, are reservoirs of biopigments that manifest diverse functionalities [34,35,36]. Carotenoids, such as lycopene, β-carotene, lutein, zeaxanthin, canthaxanthin, and astaxanthin, represent tetraterpene pigments that exhibit a spectrum of hues spanning yellow, orange, red, and purple. Carotenoids serve multifaceted biological roles, including antioxidant properties, accessory functions in photosynthesis, as well as structural and protective attributes [37]. Chlorophyll pigments, comprising chlorophyll a and b, assume a green hue and form the foundational constituents for photosynthesis [38]. Phycobiliproteins, including phycoerythrin, phycocyanin, and allophycocyanin, demonstrate fluorescent characteristics across a spectrum of colors, such as fuchsia, purple-blue, and cyan. These proteins contribute to anti-cytotoxic, apoptotic, and antioxidant functionalities, facilitating the absorption of light energy within auxiliary photosynthetic complexes [25].

Consequently, the UV–visible spectrum of microalgae is anticipated to encode rich information pertaining to their distinctive chemistry, facilitating the monitoring of microalgae production. This assertion finds validation in our findings, where discernible clustering of microalgae species was achievable in the score map. This observation underscores the notion that each species harbors a unique pigment composition, which serves as a discernible signal within the UV–visible spectrum, thereby facilitating their detection and differentiation.

In the context of microalgae cultivation, the prevailing biological contaminant of notable concern is the flagellate *Poterioochromonas malhamensis*. Its ubiquitous presence and remarkable ability to swiftly devastate entire production batches render it a significant focal point within the industrial algae sector. This flagellate specie displays a pale brown hue attributed to the presence of carotenoid fucoxanthin, predominantly localized within its chloroplast. Fucoxanthin is highly present in *P. malhamensis* and exhibits notable efficacy in light absorption and photoprotection mechanisms. In our experiments, *P. malhamensis* were fed primarily with *Chlorella*. At mixotrophic diet, *P. malhamensis* reduces fucoxanthin concentration decreasing its brown hue, and stores lipids within large lipid droplets [9]. This mechanism explains the PC2 variances depicted in Fig. 4b, wherein the loadings associated with lipids exhibit opposite influences on the scores compared to those linked to chlorophyll, consequently resulting in the distinguishable clustering of *P. malhamensis* from samples exclusively containing *Chlorella*. This observation suggests that the elevation in lipid content correlates with the reduction in chlorophyll concentration, thereby implying the presence of *P. malhamensis* as a contaminant.

Rotifers are often regarded as contaminants in microalgae cultures due to their predation on a substantial number of microalgae,

particularly species such as *Chlorella*, which are among the smallest. Rotifers, exemplified by *B. plicatilis*, range in size >100 μm and, are comparatively less abundant than microalgae in a culture. Rotifers exhibit low levels of carotenoids and lack photosynthetic pigments, rendering them nearly colorless under UV–visible light. Notably, chlorophyll originating from their microalgae diet can be detected in the stomachs of rotifers. These factors collectively pose challenges in the detection of rotifer contamination in microalgae cultures.

However, it is noteworthy that rotifers also synthesize lipids during their metabolism when preying upon microalgae. The lipid content in rotifers surpasses that of *Chlorella*, as demonstrated by the loadings of PC2 in the PCA analysis of saline sample set, as depicted in Fig. 5b. Negative loadings below 450 nm wavelengths cluster sample scores with and without rotifer contamination (see Fig. 5d and e). Additionally, negative loadings in PC3 are attributed to chlorophyll, driving the response of rotifers in the negative direction along PC3 axis. The wavelengths around the peak at 671 nm, exhibiting high negative loadings in PC3 (see Fig. 5c), correspond to chlorophyll pigment after the *Chlorella* be digested by the rotifer. In contrast, *in-vivo Chlorella* typically manifests a chlorophyll peak at 691 nm (see Fig. 2). The shift in wavelength from 691 to 671 nm can be attributed to perturbations in the energy of electronic transitions within the molecular orbitals (MO) of the chlorophyll molecule. MOs exhibit facile energy exchange with adjacent molecules and their transition energies can be significantly affected by the surrounding medium [39]. In this instance, chlorophyll molecules, post-digestion by rotifers, encounter a different environment compared to those present within *in-vivo Chlorella*, leading to this energy shift. Consequently, analysis of the chlorophyll spectrum within this spectral range can serve as an indicator of predation of *Chlorella* by some biological contaminant. This energy shift phenomenon becomes more apparent when comparing the absorption spectrum of solvent-extracted chlorophyll with that of chlorophyll within living microalgae [40,41].

Hence, despite the inherent difficulty posed by the comparatively muted coloration of flagellates and rotifers in contrast to microalgae, employing meticulous spectral data interpretation alongside appropriate machine learning, an automatic analysis can be developed based on UV–visible spectroscopy for detecting biological contaminants in microalgae cultivation. An outstanding advantage of light spectroscopy in monitoring microalgae production lies in its capability for in-line strategies or even camera-based techniques, offering a cost-effective alternative to other methods, and its simplicity in usage.

5. Conclusions

This study outlines the utilization of UV–visible spectroscopy coupled with machine learning for the analysis of aqueous microalgae cultures (*Chlorella* and *Tetradesmus*) containing biological contaminants such as *P. malhamensis* (a flagellate) and *B. plicatilis* (a rotifer). While traditionally UV–vis spectroscopy was considered less informative regarding chemical constituents compared to vibrational spectroscopies, the intricate pigment palette of the microalgae kingdom presents distinctive features within the UV–vis range. Through the analysis of UV–vis spectral data in this study, discernible chemical influences of carotenoids, chlorophylls, and lipids within the studied species were observed. These spectral patterns were effectively identified utilizing the PCA machine learning method, indicating the potential of UV–vis spectral data for classification and/or quantification purposes in real-time monitoring of microalgae cultivation concerning biological contamination. Notably, this method offers a more streamlined and cost-effective alternative to traditional approaches employed for similar purposes.

Funding

This work has received funding from the European Union – Next-GenerationEU instrument and is funded by Business Finland with grant number 6563/31/2021.

Declaration of competing interest

The authors declare that they have no known competing financial interests or personal relationships that could have appeared to influence the work reported in this paper.

Acknowledgement

The authors acknowledge Francisco Senna Vieira for producing the art of the Fig. 1 and Jenni Limnell for maintaining the organism used in this study. The work is part of the Research Council of Finland Flagship Programme, Photonics Research and Innovation (PREIN), decision number 368651.

Appendix A. Supplementary data

Supplementary data to this article can be found online at https://doi.org/10.1016/j.saa.2024.125690.

Data availability

The authors do not have permission to share data.

References

[1] P. Spolaore, C. Joannis-Cassan, E. Duran, A. Isambert, Commercial applications of microalgae, *J. Biosci. Bioeng.* 101 (2) (2006) 87–96, https://doi.org/10.1263/jbb.101.87.
[2] Y. He, et al., Comparison of fatty acid composition and positional distribution of microalgae triacylglycerols for human milk fat substitutes, *Algal Res.* 37 (2019) 40–50, https://doi.org/10.1016/j.algal.2018.11.004.
[3] T. Li, et al., A novel three-step extraction strategy for high-value products from red algae porphyridium purpureum, *Foods* 10 (9) (2021) 2164, https://doi.org/10.3390/foods10092164.
[4] J. Fabregas, C. Herrero, Vitamin content of four marine microalgae. Potential use as source of vitamins in nutrition, *J. Ind. Microbiol.* 5 (4) (1990) 259–263, https://doi.org/10.1007/BF01569683.
[5] A.K. Koyande, K.W. Chew, K. Rambabu, Y. Tao, D.-T. Chu, P.-L. Show, Microalgae: a potential alternative to health supplementation for humans, *Food Sci. Human Wellness* 8 (1) (2019) 16–24, https://doi.org/10.1016/j.fshw.2019.03.001.
[6] C. N. Kowthaman, P. Senthil Kumar, V. Arul Mozhi Selvan, and D. Ganesh, A comprehensive insight from microalgae production process to characterization of biofuel for the sustainable energy, Fuel 310 (2022) 122320, doi: 10.1016/j.fuel.2021.122320.
[7] M. Ma, D. Yuan, Y. He, M. Park, Y. Gong, Q. Hu, Effective control of Poterioochromonas malhamensis in pilot-scale culture of Chlorella sorokiniana GT-1 by maintaining CO_2-mediated low culture pH, *Algal. Res.* 26 (2017) 436–444, https://doi.org/10.1016/j.algal.2017.06.023.
[8] Z. Zhu, J. Jiang, Y. Fa, Overcoming the biological contamination in microalgae and cyanobacteria mass cultivations for photosynthetic biofuel production, *Molecules* 25 (22) (2020) 5220, https://doi.org/10.3390/molecules25225220.
[9] M. Ma, Y. Gong, Q. Hu, Identification and feeding characteristics of the mixotrophic flagellate Poterioochromonas malhamensis, a microalgal predator isolated from outdoor massive Chlorella culture, *Algal Res.* 29 (2018) 142–153, https://doi.org/10.1016/j.algal.2017.11.024.
[10] I. Moreno-Garrido, J.P. Cañavate, Assessing chemical compounds for controlling predator ciliates in outdoor mass cultures of the green algae Dunaliella salina, *Aquac. Eng.* 24 (2) (2001) 107–114, https://doi.org/10.1016/S0144-8609(00)00067-4.
[11] N.S. Ferrando, S. Nandini, M.C. Claps, S.S.S. Sarma, Effect of salinity and food concentration on competition between Brachionus plicatilis Müller, 1786 and Brachionus calyciflorus Pallas, 1776 (Rotifera), *Mar. Freshw. Res.* 71 (4) (2020) 493, https://doi.org/10.1071/MF18403.
[12] I. Maruyama, T. Nakao, I. Shigeno, Y. Ando, K. Hirayama, Application of unicellular algae Chlorella vulgaris for the mass-culture of marine rotifer Brachionus, *Hydrobiologia* 358 (1/3) (1997) 133–138, https://doi.org/10.1023/A:1003116003184.
[13] S.A. Mitchell, A. Richmond, The use of rotifers for the maintenance of monoalgal mass cultures of *Spirulina*, *Biotechnol. Bioeng.* 30 (2) (1987) 164–168, https://doi.org/10.1002/bit.260300205.
[14] V.A. Thiviyanathan, et al., Microalgae biomass and biomolecule quantification: optical techniques, challenges and prospects, *Renew. Sustain. Energy Rev.* 189 (2024) 113926, https://doi.org/10.1016/j.rser.2023.113926.
[15] L. Porras Reyes, I. Havlik, S. Beutel, Software sensors in the monitoring of microalgae cultivations, *Rev. Environ. Sci. Biotechnol.* 23(1) (2024) 67–92, doi: 10.1007/s11157-023-09679-8.

[16] J.M. Sandnes, T. Ringstad, D. Wenner, P.H. Heyerdahl, T. Källqvist, H.R. Gislerød, Real-time monitoring and automatic density control of large-scale microalgal cultures using near infrared (NIR) optical density sensors, *J. Biotechnol.* 122 (2) (2006) 209–215, https://doi.org/10.1016/j.jbiotec.2005.08.034.
[17] H. Wang, W. Zhang, L. Chen, J. Wang, T. Liu, The contamination and control of biological pollutants in mass cultivation of microalgae, *Bioresour. Technol.* 128 (2013) 745–750, https://doi.org/10.1016/j.biortech.2012.10.158.
[18] B.T. Nguyen, B.E. Rittmann, Low-cost optical sensor to automatically monitor and control biomass concentration in microalgal cultivation, *Algal Res.* 32 (2018) 101–106, https://doi.org/10.1016/j.algal.2018.03.013.
[19] P. Coltelli, L. Barsanti, V. Evangelista, A.M. Frassanito, V. Passarelli, P. Gualtieri, Automatic and real time recognition of microalgae by means of pigment signature and shape, *Environ. Sci Process Impacts* 15 (7) (2013) 1397, https://doi.org/10.1039/c3em00160a.
[20] C. Sieracki, M. Sieracki, C. Yentsch, An imaging-in-flow system for automated analysis of marine microplankton, *Mar .Ecol. Prog. Ser.* 168 (1998) 285–296, https://doi.org/10.3354/meps168285.
[21] J.-E. Thrane, et al., Spectrophotometric analysis of pigments: a critical assessment of a high-throughput method for analysis of algal pigment mixtures by spectral deconvolution, *PLoS One* 10 (9) (2015) e0137645, https://doi.org/10.1371/journal.pone.0137645.
[22] A. Malhotra, B. Örmeci, Detection and identification of a mixed cyanobacteria and microalgae culture using derivative spectrophotometry, *J. Photochem. Photobiol. B* 238 (2023) 112616, https://doi.org/10.1016/j.jphotobiol.2022.112616.
[23] X.N. He, et al., Coherent anti-Stokes Raman scattering and spontaneous Raman spectroscopy and microscopy of microalgae with nitrogen depletion, *Biomed. Opt. Exp.* 3 (11) (2012) 2896, https://doi.org/10.1364/BOE.3.002896.
[24] M.M. Olaueson, P.M. Stokes, Responses of the acidophilic alga euglena mutabilis (euglenophyceae) to carbon enrichment at pH 3, *J. Phycol.* 25 (3) (1989) 529–539, https://doi.org/10.1111/j.1529-8817.1989.tb00259.x.
[25] J. Dagnino-Leone, et al., Phycobiliproteins: Structural aspects, functional characteristics, and biotechnological perspectives, *Comput. Struct. Biotechnol. J.* 20 (2022) 1506–1527, https://doi.org/10.1016/j.csbj.2022.02.016.
[26] A.R. Ganesan, M. Shanmugam, Isolation of phycoerythrin from Kappaphycus alvarezii: a potential natural colourant in ice cream, *J. Appl. Phycol.* 32 (6) (2020) 4221–4233, https://doi.org/10.1007/s10811-020-02214-0.
[27] A. Bayu, D.R. Noerdjito, S.I. Rahmawati, M.Y. Putra, S. Karnjanakom, Biological and technical aspects on valorization of red microalgae genera Porphyridium, *Biomass Convers. Bioref.* 13 (14) (2023) 12395–12411, https://doi.org/10.1007/s13399-021-02167-5.
[28] Y.-C. Yeh, T. Ebbing, K. Frick, U. Schmid-Staiger, B. Haasdonk, G.E.M. Tovar, Improving determination of pigment contents in microalgae suspension with absorption spectroscopy: light scattering effect and bouguer–lambert–beer law, *Mar. Drugs* 21 (12) (2023) 619, https://doi.org/10.3390/md21120619.
[29] E.L. Ashenafi, M.C. Nyman, J.T. Shelley, N.S. Mattson, Spectral properties and stability of selected carotenoid and chlorophyll compounds in different solvent systems, *Food Chem. Adv.* 2 (2023) 100178, https://doi.org/10.1016/j.focha.2022.100178.
[30] M.A. Saraiva, Interpretation of α-synuclein UV absorption spectra in the peptide bond and the aromatic regions, *J. Photochem. Photobiol. B* 212 (2020) 112022, https://doi.org/10.1016/j.jphotobiol.2020.112022.
[31] H. Saber, H.R. Galal, M. Abo-Eldahab, E. Alwaleed, Enhancing the biodiesel production in the green alga Chlorella vulgaris by heavy metal stress and prediction of fuel properties from fatty acid profiles, *Environ. Sci. Pollut. Res.* 31 (24) (2024) 35952–35968, https://doi.org/10.1007/s11356-024-33538-w.
[32] H. Motahari, S.S. Mousavi, P. Haghighi, Raman, FTIR, and UV–Vis spectroscopic investigation of some oils and their hierarchical agglomerative clustering (HAC), *Food Anal. Methods* 16 (7) (2023) 1237–1251, https://doi.org/10.1007/s12161-023-02481-w.
[33] M. Didham, V.K. Truong, J. Chapman, D. Cozzolino, Sensing the addition of vegetable oils to olive oil: the ability of UV–VIS and MIR spectroscopy coupled with chemometric analysis, *Food Anal. Methods* 13 (3) (2020) 601–607, https://doi.org/10.1007/s12161-019-01680-8.
[34] E.S. Jin, A. Melis, Microalgal biotechnology: carotenoid production by the green algaeDunaliella salina, *Biotechnol. Bioprocess Eng.* 8 (6) (2003) 331–337, https://doi.org/10.1007/BF02949276.
[35] A. Bricaud, H. Claustre, J. Ras, K. Oubelkheir, Natural variability of phytoplanktonic absorption in oceanic waters: influence of the size structure of algal populations, *J. Geophys. Res. Oceans* 109 (C11) (2004), https://doi.org/10.1029/2004JC002419.
[36] L.A. Clementson, B. Wojtasiewicz, Dataset on the in vivo absorption characteristics and pigment composition of various phytoplankton species, *Data Brief* 25 (2019) 104020, https://doi.org/10.1016/j.dib.2019.104020.
[37] M. Gong, A. Bassi, Carotenoids from microalgae: a review of recent developments, *Biotechnol. Adv.* 34 (8) (2016) 1396–1412, https://doi.org/10.1016/j.biotechadv.2016.10.005.
[38] H. Scheer, Chlorophylls: a personal snapshot, *Molecules* 27 (3) (2022) 1093, https://doi.org/10.3390/molecules27031093.
[39] S.L. Ustin, et al., Retrieval of foliar information about plant pigment systems from high resolution spectroscopy, *Remote Sens. Environ.* 113 (2009) S67–S77, https://doi.org/10.1016/j.rse.2008.10.019.
[40] F.A. Almomani, B. Örmeci, Monitoring and measurement of microalgae using the first derivative of absorbance and comparison with chlorophyll extraction method, *Environ. Monit Assess* 190 (2) (2018) 90, https://doi.org/10.1007/s10661-018-6468-y.
[41] V. Domenici, D. Ancora, M. Cifelli, A. Serani, C.A. Veracini, M. Zandomeneghi, Extraction of pigment information from near-UV vis absorption spectra of extra virgin olive oils, *J. Agric. Food Chem.* 62 (38) (2014) 9317–9325, https://doi.org/10.1021/jf503818k.